Revealing the Latent Atomic World Through Data-Driven Microscopy

Steven R. Spurgeon[1, 2], Kayla Yano[1], Christina Doty[3], Sarah Akers[3], and Matthew Olszta[1]

[1] Energy and Environment Directorate, Pacific Northwest National Laboratory

[2] Department of Physics, University of Washington

[3] National Security Directorate, Pacific Northwest National Laboratory

Many emerging technologies depend on the precise design of materials structure, chemistry, and defects. As devices shrink, manufacturing tolerances tighten, and performance envelopes improve, we must increasingly measure and manipulate materials at or near the single atom level. Here we describe how transmission electron microscopy (TEM) underpins our ability to see and direct the latent atomic world. We review a selection of our recent high-resolution TEM studies of the synthesis of oxide-based nanomaterials and their evolution in extreme environments. We then discuss powerful new artificial intelligence (AI) and machine learning (ML) approaches we have developed for rich, reproducible, and scalable experimentation. We conclude by discussing future developments that will enable new materials for breakthrough technologies.

Introduction

Mastery of emerging technologies ranging from quantum computing to energy storage depends on our ability to precisely control materials at ever smaller length scales [1-3]. The central tenet of materials science is that the hierarchy of structure and chemistry – from the atomic to the macroscale – gives rise to properties and determines functionality [4, 5]. Traditionally, low-resolution processing and characterization approaches have been sufficient to incrementally improve materials performance. However, today's high performance materials contain active device regions encompassing just a handful of atoms, necessitating both exceptional resolution and precision throughput in synthesis and processing. For example, the active layers of modern transistors are now single nanometer scale [6, 7], while emerging donor qubits for quantum computing operate on the basis of single donor impurity atoms [1]. As we seek to further improve performance, we must move toward increasingly powerful ways to measure and manipulate materials.

With this goal in mind, the materials community has developed increasingly elaborate synthesis methods and approaches to observe materials in near-operating conditions [3, 8-10]. Synthesis of nanomaterials can be conducted using a variety of approaches, with some of the most powerfully precise being chemical and physical vapor deposition techniques [11, 12]. These approaches are particularly well suited to crafting precise, small volumes of materials such as thin films for electronic, optical, and magnetic devices. Molecular beam epitaxy (MBE) and pulsed laser deposition (PLD), for example, enable exquisite control of reactants to achieve a desired synthesis product. However, these methods are highly nonequilibrium in nature due to kinetic limitations, substrate effects, and the energetics of adsorbed species, often resulting in significant deviations from idealized target structures [13, 14].

Atomically precise characterization thus plays an important role in benchmarking, interpreting, and providing critical insight into materials synthesis processes [2]. Furthermore, such characterization is essential to understand ordering mechanisms, defect formation, and phase transformations, all of which give rise to emergent properties.

There are few methods that can rival the ability of electron microscopy to simultaneously probe materials structure, chemistry, and defects at high spatial resolution. Over the past several decades, transmission electron microscopy (TEM) has emerged as a cornerstone of materials science, providing an unparalleled window into the formation of materials, including property-defining defects [15, 16], the nature of order-disorder phase transitions [2, 17], and the emergence of local electronic and magnetic order [18-20]. Strongly interacting electron probes offer high-resolution insight into crystallography, composition, bonding, phase, kinetics, and electromagnetic response, often simultaneously [3, 21, 22]. The proliferation of aberration-correction, increasingly stable and powerful instrument platforms, and advanced in situ capabilities has cemented the role of this "synchrotron in a box" in laboratories worldwide [23-26]. With every successful material mystery unraveled with TEM, there are also opportunities for development. Alongside the steady pace of hardware innovations, the proliferation of artificial intelligence (AI) and machine learning (ML) in other scientific domains has begun to spill over into microscopy [27-31]. AI/ML agents that can tirelessly and effectively detect latent associations in high volume data streams are beginning to replace slow and difficult to reproduce manual approaches [32, 33]. More importantly, self-driving instrumentation is now becoming possible through the use of programmable instrument controllers [34-36] and human-like ML reasoning [37-39]. These methods will allow us to finally harness the full array of rich data at our disposal, unlocking previously impossible

experimentation across spatial, chemical, and temporal scales.

Here we review a selection of our recent high-resolution and AI-guided electron microscopy studies of the synthesis, emergent properties, and evolution of nanomaterials. We discuss prior analytical successes driven by cutting-edge hardware developments and the potential for self-driving, autonomous microscopy based on reconfigurable, centralized instrument controllers. We show how multimodal, physics-based microscopy can reveal powerful new insights into materials formation, property-defining defects, and the interaction of energy with matter. We conclude with a discussion of emerging ML capabilities for intelligent analytics, control, and forecasting. We argue that these developments are propelling electron microscopy and materials science into a more reproducible and informative era.

Discussion

We have organized this focused review into four topical areas, with a particular emphasis on the design and behavior of oxide-based nanomaterials. These materials play a critical role in technologies ranging from quantum information science to energy storage, and their lessons are generalizable to all classes of materials. First, we focus on precision design of functional oxides, which is extremely challenging due to the highly nonequilibrium nature of the associated synthesis approaches. Next, we describe efforts to understand the processing and degradation of oxides, which find use in extreme environments of deep space, nuclear reactors, and high temperatures. We then describe our efforts to create an atomic taxonomy via sparse data analytics, which are particularly well suited to electron microscopy. Finally, we discuss our platform for automated scanning TEM (STEM) utilizing a task-based, centralized communications platform. We explore the possibility of incorporating human-like reasoning into automated experiments and comment on the emerging autonomous future of microscopy.

A. Understanding the Emergence of Order in Thin Film Oxides

Many of today's most important technologies depend on precise control of oxide thin film materials. Their unique structure and chemistry give rise to important properties, such as catalytic behavior, conductivity, and magnetism [40, 41]. However, the synthesis of oxide interfaces is often kinetically limited and subject to substrate constraints, leading to many deviations from ideal, target structures. Our ability to achieve specific functionality thus depends on measuring and understanding synthesis products at high spatial and chemical resolution, a task uniquely suited to STEM. Here we consider two examples of prior work in this area, including understanding dynamic rearrangement during growth and nanoscale phase separation.

Oxide thin film synthesis takes place in complex conditions of elevated temperature (500 – 1200 °C), energetic adatom species, and highly reactive oxygen environments. Precise control of synthesis products depends on our ability to understand dynamic structural and chemical rearrangements, which are known to occur in many systems [14, 42]. This rearrangement is exemplified by our prior studies of heterojunctions of polar / non-polar $LaFeO_3$ (LFO) / $SrTiO_3$ (STO), which represents a potentially valuable system for photochemical water splitting [13, 43]. Past work has shown that the termination of the LFO / STO interface affects its band structure and resulting catalytic activity [44]. However, preparation of different terminations of STO (either SrO- or TiO_2-terminated), followed by MBE growth of LFO, results in very similar electronic structures for the final interface. To investigate this behavior, we examined the final heterojunctions using high-resolution STEM. As shown in **Figure 1**, STEM can directly resolve the excellent quality and crystallinity of the resulting interface. In particular, we observed similar profiles for chemical intermixing and no extended structural defects in either case. Using electron energy loss spectroscopy (EELS), we were able to examine the

---

Fig. 1 Dynamic Interface Rearrangement.
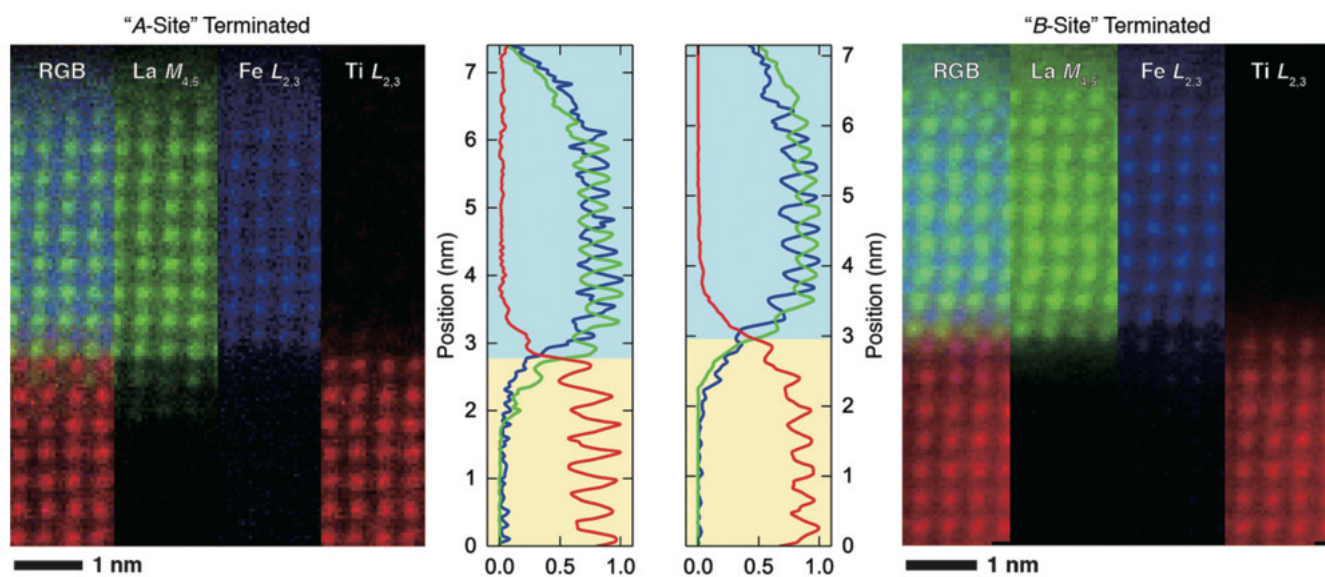
Cross-sectional EELS analysis of $LaFeO_3$ grown on two different starting surfaces of $SrTiO_3$ results in very similar final heterostructures due to dynamic rearrangement. Reproduced from Spurgeon *et al*. [13] with permission of the American Physical Society.

behavior of various alloying elements, finding that in both cases the final heterojunction assumes a LaO / TiO$_2$ configuration. EELS provides rich information on projected local density of states, as it probes inelastic core loss transitions encountered by the incident electron wave as it passes through the crystal. This measurement informed density functional theory (DFT) calculations, which indicated that the formation of a FeO$_2$ / SrO configuration was energetically quite unfavorable. Our calculations suggested that, under the growth conditions used, Sr dissolution into the bulk of the film could lead to rearrangement of the interface. In essence, despite having two distinct starting states, the end product was the same. These measurements showcase the strength of STEM to simultaneously resolve structure and chemistry, unlocking local mechanisms to guide more precise synthesis.

While structural and chemical defects are often concentrated at interfaces, they may also emerge later in growth. For example, the buildup of strain imparted by a substrate in a growing material can lead to eventual defects in the form of misfit dislocations or phase separation [45]. Alternatively, the buildup of charge associated with polar / non-polar interfaces may also drive materials to undergo nanoscale phase separation, as shown for nickelate oxides [46]. Observation of such phase separation is challenging using conventional X-ray diffraction (XRD) approaches, which lack sufficient lateral spatial and chemical resolution to uniquely identify local and aperiodic defect configurations. We examined this behavior in the double perovskite La$_2$MnNiO$_6$ (LMNO) on STO, which exhibits valuable magnetic properties directly tied to cation ordering and phase purity [15, 47]. We initially observed that ordering in this material was strongly influenced by the incorporation of oxygen during growth; the presence of oxygen vacancies can, in turn, affect cation ordering and magnetic properties. However, upon more detailed investigation, we observed the onset of nanoscale phase separation 1–5 nm into the growth. As shown in **Figure 2**, these regions exhibit a unique lattice-matched structure and appear to consist of largely NiO that has separated

from the LMNO matrix. From STEM annular bright field (ABF) imaging, it is possible to resolve the direct atomic configuration of both light and heavy elements between precipitate and matrix, yielding rich insight into the defect formation process. These observations again informed DFT calculations, which suggested that the buildup of a polar discontinuity during growth leads to initial phase pure growth, followed by phase separation into NiO. Importantly, using local STEM, we are able to effectively detect the presence of these defects, measure their spatial distribution, and determine their configuration to build more accurate models for the synthesis process.

B. Charting the Processing of Nanostructured Materials

Beyond simply synthesizing nanostructured oxides, it is also important to understand their processing and evolution in complex and extreme operating conditions. Many technologies, ranging from solid oxide fuel cells (SOFCs) to sensors and spacecraft, expose materials to extreme environments of temperature, pressure, and irradiation. Thin film oxides represent an excellent testbed to explore the coupling between processing, defects, and functionality, but they have previously received little attention. STEM analysis again provides an excellent probe to examine the unique characteristics of local environments that mediate the interaction of the host lattice with outside radiation. Here we review two examples of our prior work in this area, examining the role of interface configuration on radiation response and dynamic percolation of disorder in these materials.

As already discussed, interface configurations play an important role in determining the functionality of thin film heterostructures. These regions of a material often contain distinct structures, chemistries, and defects that mediate properties. While interfaces have been widely studied in metals by the radiation effects community as potential sources and sinks of radiation-induced defects [48], model oxide interfaces have received far less attention. We have and others have

---

Fig. 2 Nanoscale Phase Separation.
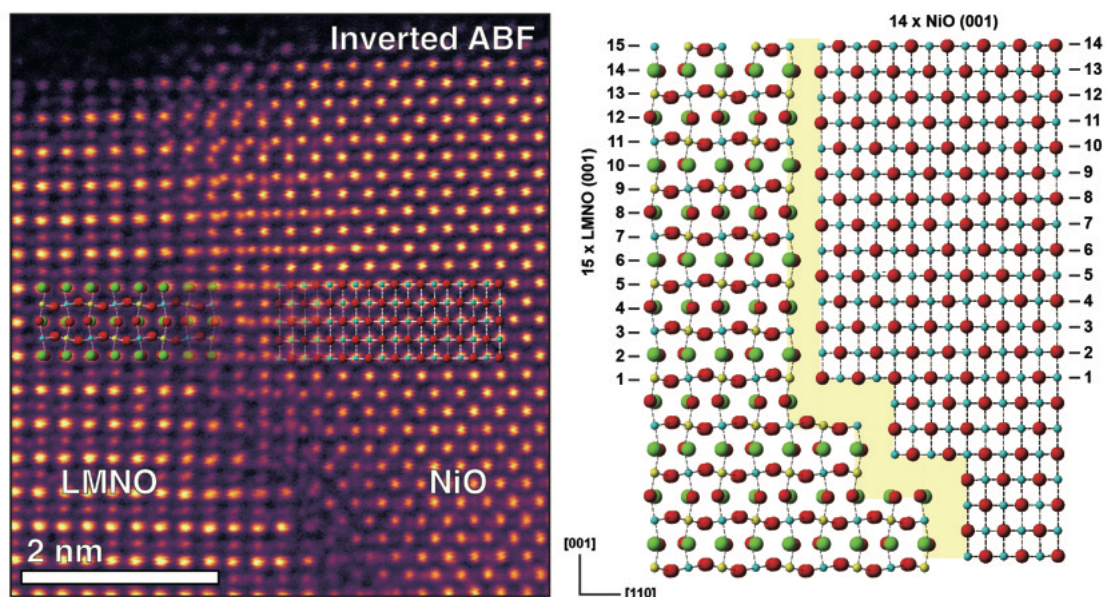
Charge buildup during the growth of La$_2$MnNiO$_6$ double perovskites leads to nanoscale NiO phase separation, as measured by inverted STEM annular bright field, leading to a solution for the interface configuration. Adapted from Spurgeon *et al*. [15] with permission of the American Physical Society.

studied the unique behavior of pyrochlore oxide interfaces [49-51], which are useful in both devices and nuclear waste storage. In particular, we have examined the $La_2Ti_2O_7$ (LTO) system grown on STO and subjected it to controlled ex situ ion irradiation with 1 MeV Zr^+ ions. Using high-resolution STEM imaging and diffraction, we are able to assess the spatial evolution of radiation damage in these materials. As shown in **Figure 3**, we observe extensive amorphization in the bulk of the film and substrate, but also the preservation of a distinct crystalline interface region in these materials. We utilized EELS to probe the chemical environment associated with radiation-induced defects in the vicinity of the interface. Our measurements showed the formation of extensive oxygen vacancies, as manifested by changes in the Ti $L_{2,3}$ and O K edge fine structure, despite the appearance of crystalline order. These findings informed DFT calculations for the energy of formation of defects for different interface configurations. In particular, our modeling showed that the interface has a higher energetic barrier to form oxygen vacancies than the bulk of either LTO film or STO substrate, suggesting that it will be last to disorder, in agreement with our experimental observations. These findings highlight the important role of interface configurations in mediating not just properties, but also radiation response and lifecycle of functional materials.

While ex situ studies of irradiation are powerful, it is well known that the evolution of radiation induced defects is highly transient and that studies of end products provides only partial mechanistic insight [8, 52, 53]. Much of our understanding of radiation effects in nanomaterials can be improved by real-time observation of defect evolution [54]. To address this gap, we examined a model $LaMnO_3$ (LMO) / STO system using the I^3TEM system at Sandia National Laboratories. This microscope is a highly modified JEOL JEM-2100 TEM, with the capability of introducing a MeV-energy level ion irradiation source in situ. In contrast to the polycrystalline or nanostructured materials commonly examined using this microscope, model thin film

oxides provide a controlled interfacial structure that can be precisely oriented relative to the ion beam.

As shown in **Figure 4**, high-resolution TEM (HRTEM) can be used to visualize the starting interface and its progression under irradiation over approximately 40 minutes to a total fluence of 6.25×10^{14} Au^{4+} cm^{-2}. We examined raw images and also measured changes in crystallinity, using time-resolved Fourier filtering of Bragg reflections corresponding to the film lattice planes. This approach allowed us to visualize the initial, largely crystalline microstructure and the percolation of disorder in the vicinity of the interface. We observed that disorder first emerges at the center of the LMO film, in the form of local dislocations, and subsequently progresses to the film-substrate interface. The initial rate of disorder is slow, with just 5% of crystallinity lost in the first 5 minutes, but it soon accelerates to nearly 15% loss between 9 − 19 minutes. At this point, the disorder appears to plateau, with a further drop in crystallinity by 40% at the end of 40 minutes. Our direct observations revealed a complex percolation and breakup of the material, beginning away from the interface and progressing toward it. These results again informed DFT calculations of defect energies, which showed the propensity for LMO to disorder before STO, as observed experimentally. More broadly, these results speak to the powerful local information that in situ TEM can provide, helping us to understand the dynamic evolution of materials in extreme environments.

C. Building the Atomic Taxonomy

As the preceding sections have shown, today's microscopes are capable of generating immense volumes of simultaneous multimodal imaging, spectroscopic, and diffraction data. However, it is presently difficult for us to fully harness and act on such data using conventional analysis approaches, which cannot scale and are prone to irreproducibility because of their human-in-the-loop design. ML methods can potentially analyze data in a more reproducible, holistic, and semantically meaningful way to

---

Fig. 3 Chemical Analysis of Interfacial Disorder.
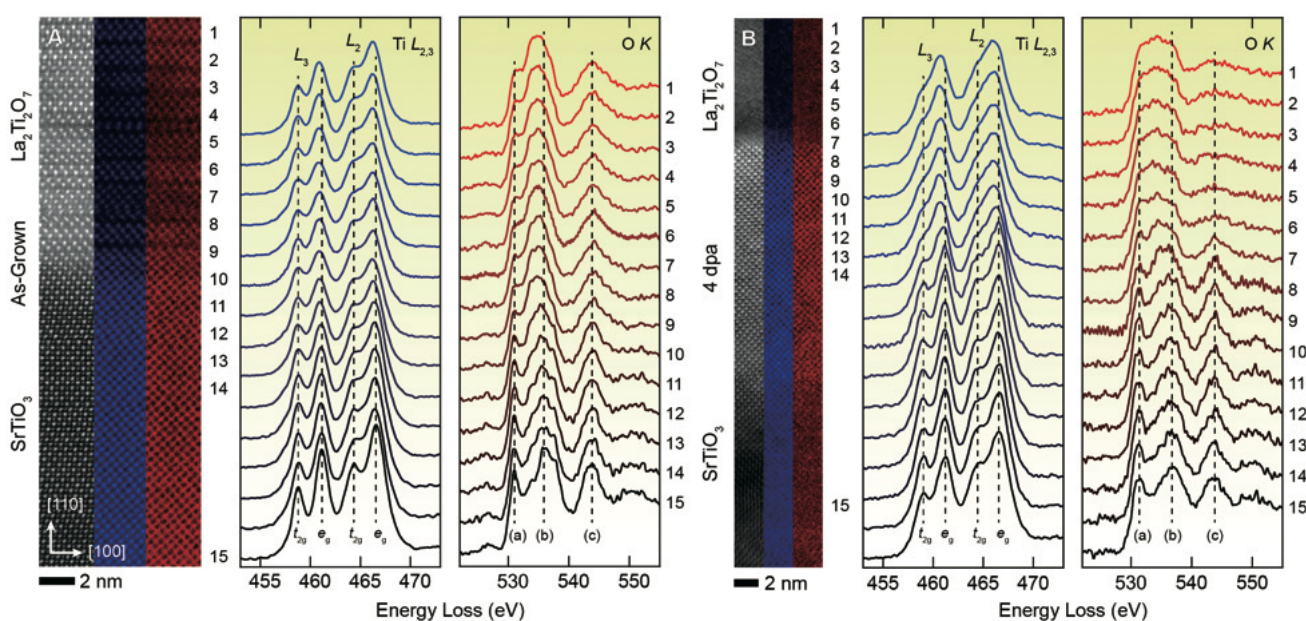
EELS measurements of an $La_2Ti_2O_7$ / $SrTiO_3$ interface before (A–C) and after (D–F) irradiation, showing both the preservation of an interfacial crystalline region and formation of extensive oxygen vacancies. Adapted from Spurgeon *et al*. [49] under CC.-BY-4.0 license.

extract relevant materials descriptors [27, 30, 33]. Until recently, these methods have been developed in other domains, and they lack tuning to make them suitable for electron microscopy. We must consider specific characteristics of microscopy data, including data sparsity, a lack of high-quality training data, noisy acquisitions, and the strong dependence of the imaging function on instrument parameters.

We have specifically chosen to address the challenge of data sparsity, which is a major barrier to the adopt of ML in microscopy. As convolutional neural network (CNN) algorithms continue to push computer vision (CV) tasks to unprecedented performance, the community has begun to realize that these data hungry models are difficult or impossible to implement in scientific domains [56]. The high cost of data annotation [57], necessary for model training, creates a brittleness in traditionally trained architectures that causes performant models to fail on out-of-distribution samples. Specifically, there is a need for high-performance models that can accommodate real-world scenarios with few to no annotations. This need has led to development of few-shot learning approaches, which rely on an extremely limited amount of prior information—even one or two data points [58, 59]. The ability to analyze data sets in the presence of limited training data, as is the case for transient, unstable, or novel materials, is an important frontier in materials and data science [32]. As shown in **Figure 5**.A, we have recently developed a flexible few-shot approach that leverages the sparse labeling paradigm to quickly describe and locate regions in electron micrographs [39]. In this approach, a larger microstructure is first broken down into semantically meaningful features known as chips, which may encompass atomic-scale motifs, particles, or grains, for example. These chips are passed through a previously trained encoder and then compared against canonical examples via a metal earner. The result is a chip level and task-based segmentation of the image, with associated statistics on classes of interest. This model does not require any retraining between tasks and can be effectively scaled to large volumes of data. Most importantly, the model can be quickly adapted to account for new information, taking mere seconds to select new support sets, compared to hours of traditional hand labeling.

Alongside this model, we have developed an intuitive graphical user interface (GUI) to aid in training and applying a model to new data sets, as shown in Figure 5.B. Often, research is primarily focused on model development but not its actual deployment into day to day workflows. The best case scenario at present is typically a Jupyter Notebook or Google Collab distribution. However, these implementations are often difficult to use due to complicated dependencies, their notebook-style execution, and poor runtime performance. A GUI can improve model trustworthiness and explainability, as the images displayed at each stage of the model's training and inference are easily interpreted by a microscopist, and can give much needed context to values such as accuracy and uncertainty [60]. While our model only requires a few examples of each feature type, there are several preprocessing steps that must be performed to prepare these example sets [39]. One step involves identifying a good chip size based on the size of features in the image. The GUI eliminates the trial- and-error in this step by providing the user with a slider, which dynamically updates the size of a grid of chips overlaid on top of their image. Another step involves identifying the location of feature examples within the image. The GUI facilitates this by allowing the user to click on a chip containing a feature to add it to (or remove it from) an example set [60]. This GUI significantly improves the accessibility of the few-shot model to microscopists, while increasing its

Fig. 4 Nanoscale Percolation of Disorder.
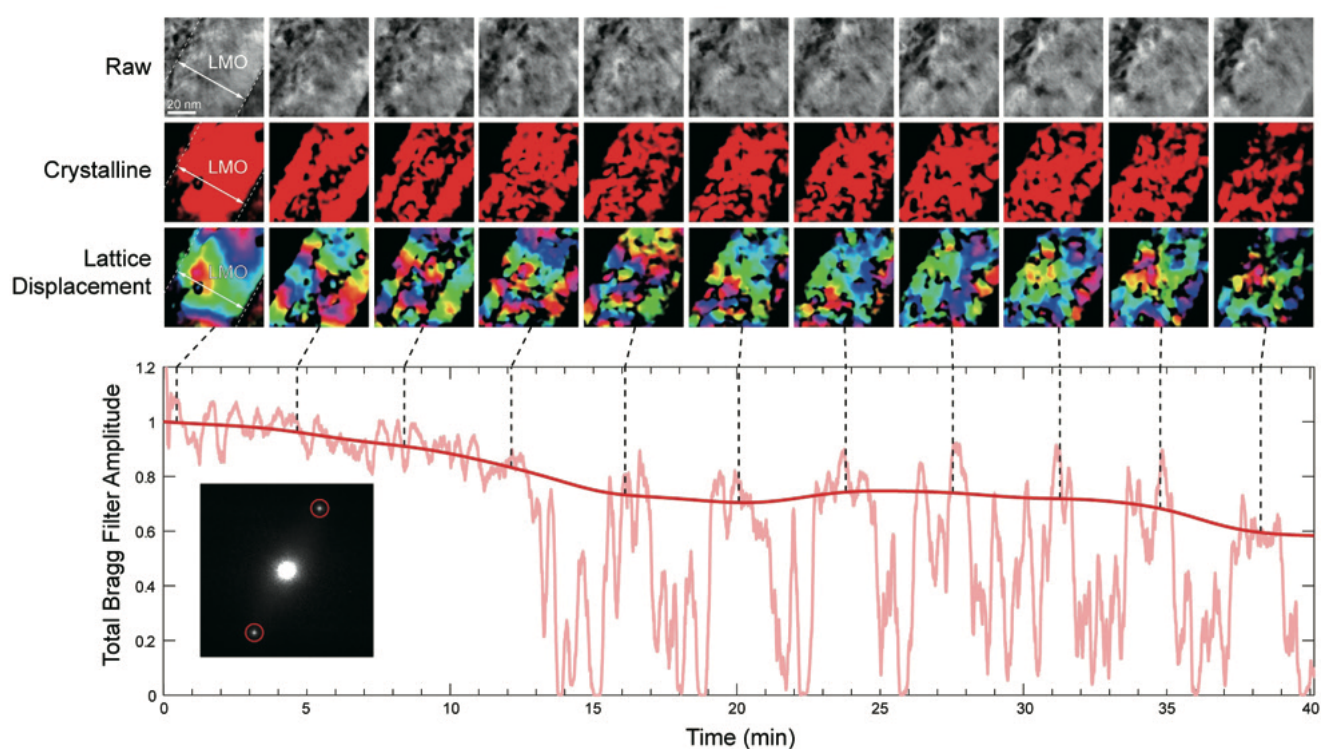
In situ HRTEM and time-resolved Fourier filtering reveal pathways for disorder during irradiation of LaMnO$_3$ / SrTiO$_3$ interfaces. Reproduced from Matthews *et al.* [55] under CC.-BY-4.0 license.

Fig. 5 Sparse Analytics for Material Descriptors.
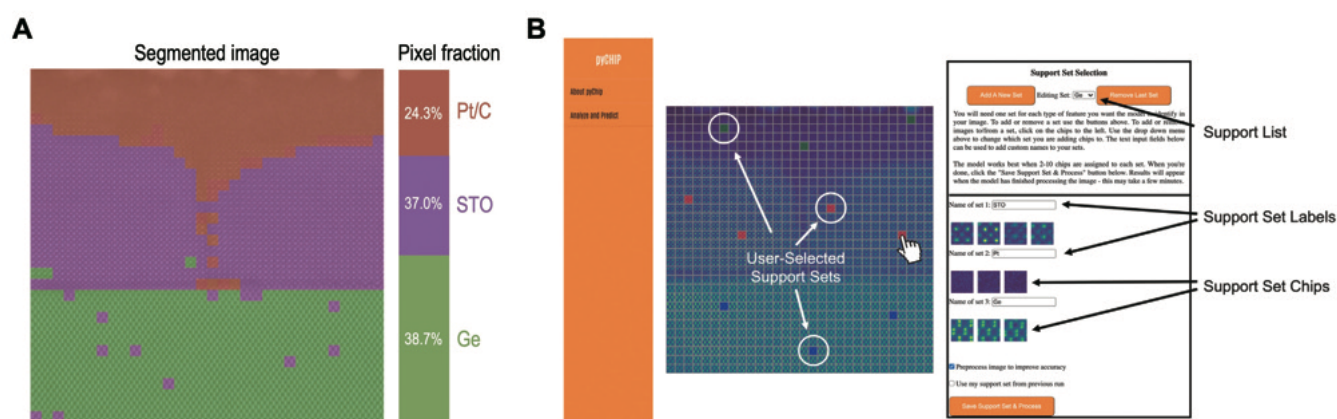
Emerging few-shot ML can rapidly perform triaging and classification of SrTiO$_3$ / Ge interfaces by task (A), using a GUI that enables dynamic and transparent model operation (B). Adapted from Akers *et al*. [39] and Doty *et al*. [60] under CC.-BY-4.0 license.

interpretability and explainability.

The ability to curate large amounts of data is one facet of next-generation electron microscopy, but copious data without informed collection is also a valid concern, especially when machine learning algorithms are based upon user-provided ground truth. Our research group has developed the protocols coined Nanocartography, which provides microscopists with a toolbox to bridge the gap between reciprocal space and real space [61-64]. As previously noted, control of the stage has often been an overlooked feature in the materials electron microscopy community, most likely owing to the highly site-specific nature of sample analysis. Predictive and precision control of the stage is necessary for performing large area montaging, but as well for tilting experiments. Coupling tilting in real space (e.g., morphological examinations and interfaces) to reciprocal space (diffraction) provides microscopists with the ability accurately plan and direct microstructural and microchemical examinations. It has long been known that investigation of grain boundaries is highly dependent upon correct orientation whether towards the appropriate detector [65]. Nanocartography provides the ability to intelligently assess crystallographic orientation with respect to the physical features within a sample as well as the stage. Knowledge of these relationships also allows for rapid re-analysis of samples because orientation can be recalled. Automation of oblique tilt series (i.e., tilt series where the feature of interest is not aligned with the alpha or beta axis) can be programmed to assess three dimensional nature of the sample without destructive analysis and other limitations of full tomography. Finally, adoption of this protocol will promote collaboration between labs, since users can readily share mapping information of various samples, thereby reducing expensive costs associated with re-exploration of existing samples.

D. Moving Toward the Autonomous Future

With the convergence of high-resolution analysis capability and bespoke ML, we are now increasingly moving toward completely automated, AI-guided microscope architectures [31, 35]. As already discussed, models that replicate human-like reasoning are only one part of these architectures; we must also develop centralized controllers to collect data and implement decision-making. As an example, we can consider automated montaging

of large statistical volumes of material, which is useful for understanding synthesis products, failure mechanisms, and the evolution of materials in situ. At its simplest, automated montaging should provide a scientist user with modifiable settings to dictate the number of images to be taken over a given area. While this technology exists on other instruments, such as scanning electron microscopes (SEMs), arbitrary task-based, self-driving montaging is presently unavailable in the STEM.

To address this challenge, we have developed an automated instrument architecture called AutoEM based on asynchronous, centralized control of a JEOL GRAND ARM™ (JEM-ARM300F) STEM instrument [35]. We implement a new low-level Python application programming interface (API), called pyJEM, which allows us to both issue instrument commands and read out data [66]. As shown in **Figure 6**, this platform enables various new automated analysis modes. We consider an example analysis of MoO$_3$ nanoparticles, a transition metal oxide of significant interest as an energy storage material, photocatalyst, and adsorbent due to its tunable nanostructure [67]. The ability to synthesize desired morphologies (typically plates or rods) is essential, as large surface areas play a key role in catalysis, and statistical analysis can inform improved nanoparticle processing. In open-loop experimentation (Figure 6.A), a user can identify an area of interest and the automated platform will image this region, sending over the final montage to a few-shot ML model trained to distinguish particle features. At this point, the model can branch to different tasks, such as distinguishing all particles from the background or distinguishing different particle types (Figure 6.B). Finally, the system can automatically identify and drive to features of interest determined by the few-shot analysis, as shown in Figure 6.C. AutoEM allows for increased throughput, repeatability, and improved statistics over manual data collection, informing important synthesis and processing outcomes.

Equipped with a centralized instrument controller, we can now implement more sophisticated ML analytics for on-the-fly decision-making during in situ studies. We have recently explored predictive ML for forecasting of chemical reactions in the microscope. Based on a type of recurrent neural network (RNN), long short-term memory models (LSTMs) have found use in prediction of video data [68]. Despite their power, these models have not yet been applied to in situ reactions in the TEM, where they might inform automated decision-making. We have developed a specialized LSTM model for EELS data,

called EELSTM, that allows us to predict the future state of real-time reduction of STO [69]. As shown in **Figure 7**, this model can describe an entire core-loss EELS spectrum with exceptional accuracy relative to ground truth experimental data. Since the core-loss region encodes information about oxidation state and bonding, it is a powerful indicator of local defects formed at different stages of materials processing [9]. EELSTM uses prior spectra to predict a future spectrum and could provide necessary predictive capabilities for automated instrument control in AutoEM. Alternatively, this model may be used to artificially run reactions to completion to further augment the temporal resolution of a given experiment. More broadly, this model shows the power of the modular AutoEM system to incorporate various analytic engines, depending on the desired task.

Conclusions

The science of atomic-resolution electron microscopy has illuminated fundamental mechanisms for materials synthesis and processing that would otherwise go unnoticed. It has become a mainstay of modern materials science, chemistry, and physics, continuing to inform our mechanistic understanding of processes that underpin emerging technologies. As we have shown, TEM imaging, spectroscopy, and diffraction can richly probe the complex defect pathways for materials formation and degradation. These methods allow us to better understand how materials will evolve in complex, harsh operating environments, leading to improved materials design and performance lifecycles.

The field of materials science and microscopy are collectively in the midst of transformation. While previous approaches remain valuable, emerging AI/ML will reshape how scientific experimentation is conducted. Our early work has shown that machine intelligence can better harness existing data and unlock powerful new types of experiments. These approaches can lead to more accurate and comprehensive models for materials synthesis and processing. Nonetheless, it is increasingly clear that hardware developments must be accompanied by more agile and open software development. Reconfigurable and modular instrumentation ecosystems, with adaptable hardware, programmable controllers, and interchangeable analytics, represents the future of electron microscopy. These new ecosystems will improve reproducibility and permit broad dissemination of best experimental practices. Constantly updating instrumentation, informed by the latest AI/ML, will elevate the state-of-the-art more broadly and catalyze transformative discovery in the coming decade.

Fig. 6 Sparse Data-Guided Automated Microscopy.
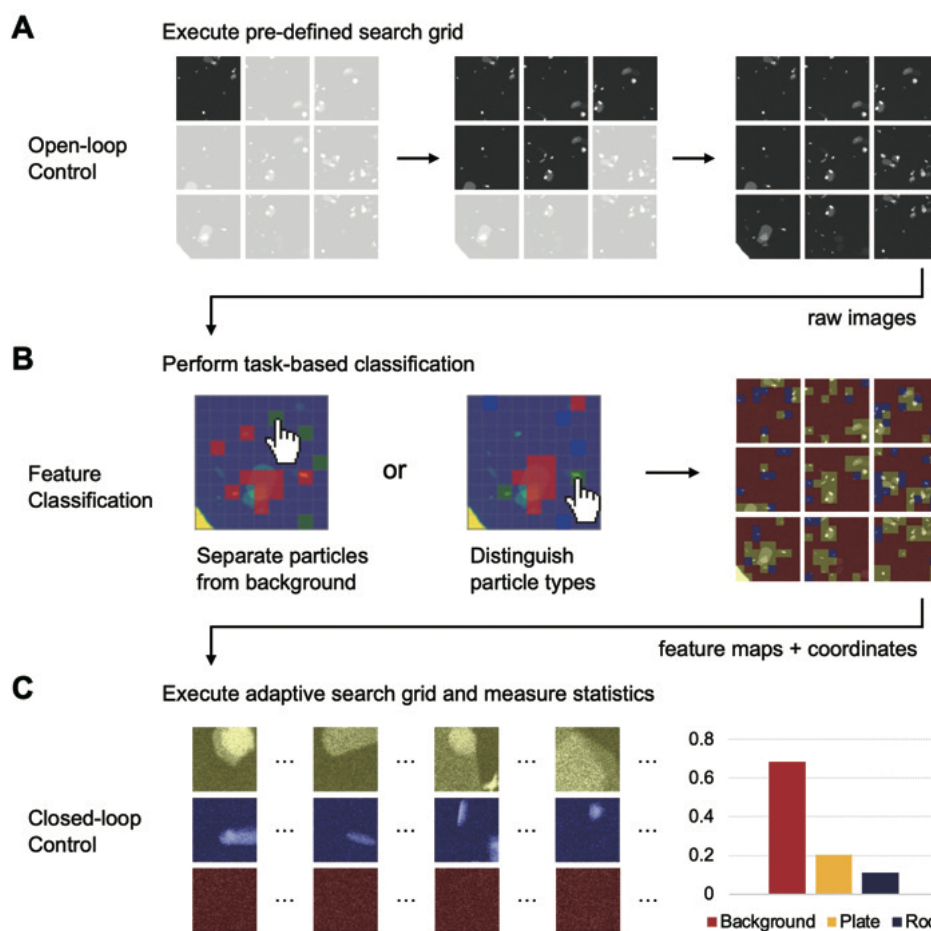
Centralized instrument control and on-the-fly analytics enable automated experimentation. (A–B) Pre-defined search grids provide statistical overviews of MoO_3 nanoparticles, which can be automatically analyzed by task. (C) Analysis results then drive adaptive searches for specific features of interest. Reproduced from Olszta *et al*. [35] under CC.-BY-4.0 license.

Fig. 7 ML-Based Forecasting of Phase Transitions.
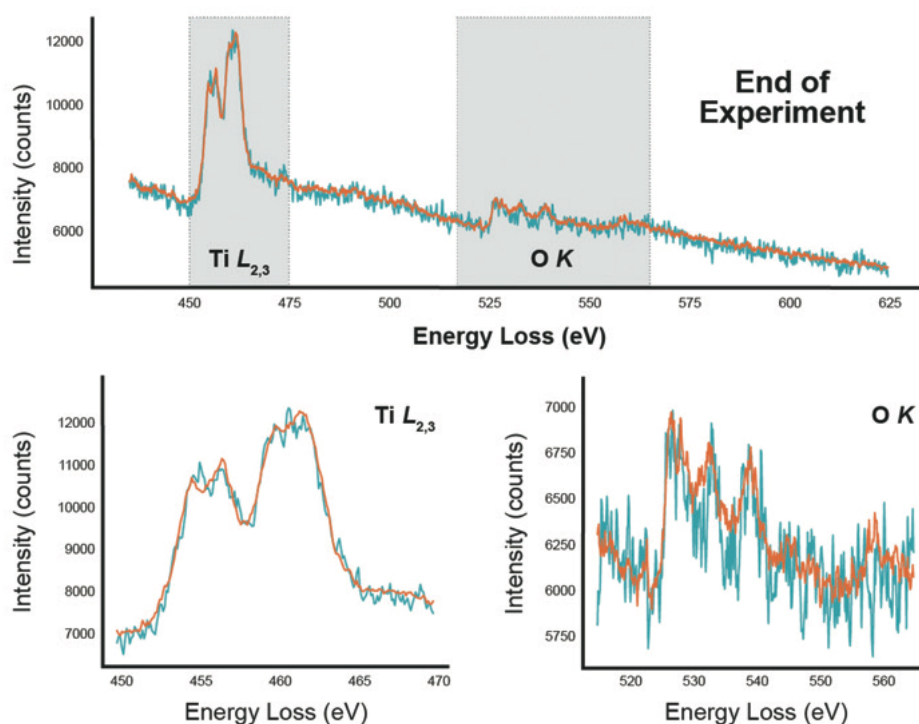
Specialized LSTM models can accurately predict the future state of reduction in SrTiO$_3$ via EELS data. The raw data (ground truth) is shown in blue and the prediction is shown in orange. Reproduced from Lewis *et al*. [69] under CC.-BY-4.0 license.

References

[1] N. P. d. Leon, K. M. Itoh, D. Kim, K. K. Mehta, T. E. Northup, H. Paik, B. S. Palmer, N. Samarth, S. Sangtawesin, and D. W. Steuerman, "Materials challenges and opportunities for quantum computing hardware," *Science* **372**, 253 (2021).

[2] S. R. Spurgeon, "Order-disorder behavior at thin film oxide interfaces," *Current Opinion in Solid State and Materials Science* **24**, 100870 (2020-12), https://linkinghub.elsevier.com/retrieve/pii/S1359028620300681.

[3] C. Zhang, K. L. Firestein, J. F. S. Fernando, D. Siriwardena, J. E. Treifeldt, and D. Golberg, "Recent Progress of In Situ Transmission Electron Microscopy for Energy Materials," *Advanced Materials* **1904094**, (2019).

[4] S. R. Kalidindi and M. D. Graef, "Materials Data Science: Current Status and Future Outlook," *Annual Review of Materials Research* **45**, 171–193 (2015-7).

[5] D. T. Fullwood, S. R. Niezgoda, B. L. Adams, and S. R. Kalidindi, "Microstructure sensitive design for performance optimization," *Progress in Materials Science* **55**, 477–562 (2010-8), https://linkinghub.elsevier.com/retrieve/pii/S0079642509000760.

[6] K. A. Brown, S. Brittman, N. Maccaferri, D. Jariwala, and U. Celano, "Machine Learning in Nanoscience: Big Data at Small Scales," *Nano Letters* **20**, 2–10 (2020).

[7] I. K. Schuller and R. Stevens, "Neuromorphic Computing : From Materials to Systems Architecture Report of a Roundtable Convened to Consider Neuromorphic Computing," Tech. Rep. (2015).

[8] R. J. Parrish, D. C. Bufford, D. M. Frazer, C. A. Taylor, J. Gutierrez-Kolar, D. L. Buller, B. L. Boyce, and K. Hattar, "Exploring Coupled Extreme Environments via In-situ Transmission Electron Microscopy," *Microscopy Today* **29**, 28–34 (2021).

[9] S. Spurgeon and S. Chambers, "Reference Module in Chemistry, Molecular Sciences and Chemical Engineering," in Encyclopedia of Interfacial Chemistry (Elsevier, New York, 2017) pp. 38–48, https://linkinghub.elsevier.com/retrieve/pii/B978012409547212877X.

[10] C. J. Palmstrøm, "Heusler compounds and spintronics," *Progress in Crystal Growth and Characterization of Materials* **62**, 371–397 (2016).

[11] M. Brahlek, A. S. Gupta, J. Lapano, J. Roth, H.-T. T. Zhang, L. Zhang, R. Haislmaier, and R. Engel-Herbert, "Frontiers in the Growth of Complex Oxide Thin Films: Past, Present, and Future of Hybrid MBE," *Advanced Functional Materials* **28**, 1–41 (2018-2).

[12] S. A. Chambers, "Epitaxial growth and properties of doped transition metal and complex oxide films," *Advanced Materials* **22**, 219–248 (2010-1).

[13] S. R. Spurgeon, P. V. Sushko, S. A. Chambers, and R. B. Comes, "Dynamic interface rearrangement in LaFeO$_3$/n-SrTiO$_3$ heterojunctions," *Physical Review Materials* **1**, 063401 (2017).

[14] J. H. Lee, G. Luo, I. C. Tung, S. H. Chang, Z. Luo, M.

Malshe, M. Gadre, A. Bhattacharya, S. M. Nakhmanson, J. A. Eastman, H. Hong, J. Jellinek, D. Morgan, D. D. Fong, and J. W. Freeland, "Dynamic layer rearrangement during growth of layered oxide films by molecular beam epitaxy," *Nature Materials* **13**, 879–883 (2014), http://doi.wiley.com/10.1002/adfm.201102763.

[15] S. R. Spurgeon, P. V. Sushko, A. Devaraj, Y. Du, T. Droubay, and S. A. Chambers, "Onset of phase separation in the double perovskite oxide La_2MnNiO_6," *Physical Review B* **97**, 134110 (2018), https://pubs.acs.org/doi/10.1021/acs.chemmater.6b00829, 1710.08535.

[16] S. A. Chambers, Y. Du, Z. Zhu, J. Wang, M. J. Wahila, L. F. J. Piper, A. Prakash, J. Yue, B. Jalan, S. R. Spurgeon, D. M. Kepaptsoglou, Q. M. Ramasse, and P. V. Sushko, "Interconversion of intrinsic defects in $SrTiO_3$ (001)," *Physical Review B* **97**, 245204 (2018).

[17] C. M. Rost, E. Sachet, T. Borman, A. Moballegh, E. C. Dickey, D. Hou, J. L. Jones, S. Curtarolo, and J.-P. Maria, "Entropy-stabilized oxides," *Nature Communications* **6**, 8485 (2015).

[18] D. G. Schlom, L.-Q. Chen, C. J. Fennie, V. Gopalan, D. a. Muller, X. Pan, R. Ramesh, and R. Uecker, "Elastic strain engineering of ferroic oxides," *MRS Bulletin* **39**, 118–130 (2014).

[19] T. Zhang, X. P. Wang, Q. F. Fang, and X. G. Li, "Magnetic and charge ordering in nanosized manganites," *Applied Physics Reviews* **031302**, 0–21 (2014).

[20] H. Y. Hwang, Y. Iwasa, M. Kawasaki, B. Keimer, N. Nagaosa, and Y. Tokura, "Emergent phenomena at oxide interfaces," *Nature Materials* **11**, 103–113 (2012).

[21] C. Colliex, "From a physicist's toy to an indispensable analytical tool in many fields of science: A personal view of the leading contribution of Ondrej Krivanek to the spectacular successes of EELS spectroscopy in the electron microscope," *Ultramicroscopy* **180**, 14–21 (2017).

[22] H. Zheng, Y. S. Meng, and Y. Zhu, "Frontiers of in situ electron microscopy," *MRS Bulletin* **40**, 12–18 (2015), https://www.cambridge.org/core/product/identifier/S0883769414003054/type/journal article.

[23] Q. M. Ramasse, "Twenty years after: How "Aberration correction in the STEM" truly placed a "A synchrotron in a Microscope"," *Ultramicroscopy* **180**, 41–51 (2017).

[24] I. MacLaren and Q. M. Ramasse, "Aberration-corrected scanning transmission electron microscopy for atomic-resolution studies of functional oxides," *International Materials Reviews* **59**, 115–131 (2014).

[25] D. a. Muller, "Structure and bonding at the atomic scale by scanning transmission electron microscopy." *Nature materials* **8**, 263–70 (2009-4).

[26] P. E. Batson, N. Dellby, and O. L. Krivanek, "Sub-ångstrom resolution using aberration corrected electron optics," *Nature* **419**, 94–94 (2002), http://www.ncbi.nlm.nih.gov/pubmed/12167855.

[27] K. P. Treder, C. Huang, J. S. Kim, and A. I. Kirkland, "Applications of deep learning in electron microscopy," *Microscopy* **71**, i100–i115 (2022).

[28] M. Xu, A. Kumar, and J. M. LeBeau, "Towards Augmented Microscopy with Reinforcement Learning-Enhanced Workflows," *Microscopy and Microanalysis*, 1–9 (2022), 2208.02865.

[29] M. Ziatdinov, A. Ghosh, C. Y. T. Wong, and S. V. Kalinin, "Atom AI framework for deep learning analysis of image and spectroscopy data in electron and scanning probe microscopy," *Nature Machine Intelligence*, 1–12 (2022).

[30] J. M. Ede, "Deep learning in electron microscopy," *Machine Learning: Science and Technology* **2**, 011004 (2021), https://iopscience.iop.org/article/10.1088/2632-2153/abd614, 2009.08328.

[31] S. V. Kalinin, M. A. Ziatdinov, J. Hinkle, S. Jesse, A. Ghosh, K. P. Kelley, A. R. Lupini, B. G. Sumpter, and R. K. Vasudevan, "Automated and Autonomous Experiment in Electron and Scanning Probe Microscopy," *ACS Nano* **15**, 1–48 (2021), 2103.12165.

[32] S. V. Kalinin, M. Ziatdinov, S. R. Spurgeon, C. Ophus, E. A. Stach, T. Susi, J. Agar, and J. Randall, "Deep learning for electron and scanning probe microscopy: From materials design to atomic fabrication," *MRS Bulletin* **47**, 931–939 (2022).

[33] S. R. Spurgeon, C. Ophus, L. Jones, A. Petford-Long, S. V. Kalinin, M. J. Olszta, R. E. Dunin-Borkowski, N. Salmon, K. Hattar, W.-c. D. Yang, R. Sharma, Y. Du, A. Chiaramonti, H. Zheng, E. C. Buck, L. Kovarik, R. L. Penn, D. Li, X. Zhang, M. Murayama, and M. L. Taheri, "Towards data-driven next-generation transmission electron microscopy," *Nature Materials* **20**, 274–279 (2021), http://www.nature.com/articles/s41563-020-00833-z.

[34] K. M. Roccapriore, M. G. Boebinger, O. Dyck, A. Ghosh, R. R. Unocic, S. V. Kalinin, and M. Ziatdinov, "Probing Electron Beam Induced Transformations on a Single-Defect Level via Automated Scanning Transmission Electron Microscopy," *ACS Nano* **16**, 17116–17127 (2022).

[35] M. Olszta, D. Hopkins, K. R. Fiedler, M. Oostrom, S. Akers, and S. R. Spurgeon, "An Automated Scanning Transmission Electron Microscope Guided by Sparse Data Analytics," *Microscopy and Microanalysis* **28**, 1611–1621 (2022), 2109.14772.

[36] M. Schorb, I. Haberbosch, W. J. Hagen, Y. Schwab, and D. N. Mastronarde, "Software tools for automated transmission electron microscopy," *Nature Methods* **16**, 471–477 (2019).

[37] Y. Liu, K. P. Kelley, R. K. Vasudevan, H. Funakubo, M. A. Ziatdinov, and S. V. Kalinin, "Experimental discovery of structure–property relationships in ferroelectric materials via active learning," *Nature Machine Intelligence* **4**, 341–350 (2022).

[38] M. Ziatdinov, Y. Liu, K. Kelley, R. Vasudevan, and S. V. Kalinin, "Bayesian Active Learning for Scanning Probe Microscopy: From Gaussian Processes to Hypothesis Learning," *ACS Nano* **16**, 13492–13512 (2022).

[39] S. Akers, E. Kautz, A. Trevino-Gavito, M. Olszta, B. E. Matthews, L. Wang, Y. Du, and S. R. Spurgeon, "Rapid and flexible segmentation of electron microscopy data using few-shot machine learning," npj *Computational Materials* **7**, 187 (2021).

[40] J. Chakhalian, J. W. Freeland, A. J. Millis, C. Panagopoulos, and J. M. Rondinelli, "Emergent properties in plane view: Strong correlations at oxide interfaces," *Reviews of Modern Physics* **86**, 1189–1202 (2014), http://link.aps.org/doi/10.1103/RevModPhys.86.1189, 1408.3173.

[41] J. Mannhart and D. G. Schlom, "Oxide Interfaces–An Opportunity for Electronics," *Science* **327**, 1607–1611 (2010), http://www.sciencemag.org/cgi/doi/10.1126/science.1181862.

[42] G. Saint-Girons, R. Bachelet, R. Moalla, B. Meunier, L. Louahadj, B. Canut, A. Carretero-Genevrier, J. Gazquez, P. Regreny, C. Botella, J. Penuelas, M. G. Silly, F. Sirotti, and G.

Grenet, "Epitaxy of SrTiO$_3$ on Silicon: The Knitting Machine Strategy," *Chemistry of Materials* **28**, 5347–5355 (2016).

[43] R. Comes and S. Chambers, "Interface structure, band alignment, and built-in potentials at LaFeO$_3$ / n-SrTiO$_3$ heterojunctions," *Physical Review Letters* **117**, 226802 (2016), https://link.aps.org/doi/10.1103/PhysRevLett.117.226802.

[44] K. Stoerzinger, R. Comes, S. Spurgeon, S. Thevuthasan, K. Ihm, E. Crumlin, and S. Chambers, "Influence of LaFeO¡sub¿3¡/sub¿ Surface Termination on Water Reactivity," *The Journal of Physical Chemistry Letters* **8**, 1038 – 1043 (2017).

[45] J. L. Macmanus-Driscoll, "Self-assembled heteroepitaxial oxide nanocomposite thin film structures: Designing interface-induced functionality in electronic materials," *Advanced Functional Materials* **20**, 2035–2045 (2010).

[46] E. Detemple, Q. M. Ramasse, W. Sigle, G. Cristiani, H.-U. Habermeier, E. Benckiser, a. V. Boris, A. Frano, P. Wochner, M. Wu, B. Keimer, and P. A. v. Aken, "Polarity-driven nickel oxide precipitation in LaNiO$_3$-LaAlO$_3$ superlattices," *Applied Physics Letters* **99**, 211903 (2011).

[47] S. R. Spurgeon, Y. Du, T. Droubay, A. Devaraj, X. Sang, P. Longo, P. Yan, P. G. Kotula, V. Shutthanandan, M. E. Bowden, J. M. LeBeau, C. Wang, P. V. Sushko, and S. A. Chambers, "Competing Pathways for Nucleation of the Double Perovskite Structure in the Epitaxial Synthesis of La$_2$MnNiO$_6$," *Chemistry of Materials* **28**, 3814–3822 (2016), http://dx.doi.org/10.1021/acs.chemmater.6b00829 http://pubs.acs.org/doi/abs/10.1021/acs.chemmater.6b00829.

[48] I. Beyerlein, A. Caro, M. Demkowicz, N. Mara, A. Misra, and B. Uberuaga, "Radiation damage tolerant nanomaterials," *Materials Today* **16**, 443–449 (2013-11), https://linkinghub.elsevier.com/retrieve/pii/S1369702113003581.

[49] S. R. Spurgeon, T. C. Kaspar, V. Shutthanandan, J. Gigax, L. Shao, and M. Sassi, "Asymmetric Lattice Disorder Induced at Oxide Interfaces," *Advanced Materials Interfaces* **7**, 1901944 (2020), https://onlinelibrary.wiley.com/doi/abs/10.1002/admi.201901944, 1904.05932.

[50] T. C. Kaspar, J. G. Gigax, L. Shao, M. E. Bowden, T. Varga, V. Shutthanandan, S. R. Spurgeon, P. Yan, C. Wang, P. Ramuhalli, and C. H. Henager, "Damage evolution of ion irradiated defected-fluorite La$_2$Zr$_2$O$_7$ epitaxial thin films," *Acta Materialia* **130**, 111–120 (2017-5), https://linkinghub.elsevier.com/retrieve/pii/S1359645417300228.

[51] T. C. Kaspar, S. Hong, M. E. Bowden, T. Varga, P. Yan, C. Wang, S. R. Spurgeon, R. B. Comes, P. Ramuhalli, and C. H. Henager, "Tuning piezoelectric properties through epitaxy of La$_2$Ti$_2$O$_7$ and related thin films," *Scientific Reports* **8**, 3037 (2018).

[52] K. Hattar and K. L. Jungjohann, "Possibility of an integrated transmission electron microscope: enabling complex in-situ experiments," *Journal of Materials Science* **56**, 5309–5320 (2021).

[53] K. Hattar, D. Bufford, and D. Buller, "Concurrent in situ ion irradiation trans- mission electron microscope," *Nuclear Instruments and Methods in Physics Research Section B: Beam Interactions with Materials and Atoms* **338**, 56–65 (2014-11), https://linkinghub.elsevier.com/retrieve/pii/S0168583X14007046.

[54] X. Zhang, K. Hattar, Y. Chen, L. Shao, J. Li, C. Sun, K. Yu, N. Li, M. L. Taheri, H. Wang, J. Wang, and M. Nastasi, "Radiation damage in nanostructured materials," *Progress in Materials Science* **96**, 217–321 (2018-7), https://linkinghub.elsevier.com/retrieve/pii/S007964251830032X.

[55] B. E. Matthews, M. Sassi, C. Barr, C. Ophus, T. C. Kaspar, W. Jiang, K. Hattar, and S. R. Spurgeon, "Percolation of Ion-Irradiation-Induced Disorder in Complex Oxide Interfaces," *Nano Letters* **21**, 5353–5359 (2021).

[56] N. Fujinuma, B. DeCost, J. Hattrick-Simpers, and S. E. Lofland, "Why big data and compute are not necessarily the path to big materials science," *Communications Materials* **3**, 59 (2022).

[57] R. Sainju, W.-Y. Chen, S. Schaefer, Q. Yang, C. Ding, M. Li, and Y. Zhu, "DefectTrack: a deep learning-based multi-object tracking algorithm for quantitative defect analysis of in-situ TEM videos in real-time," *Scientific Reports* **12**, 15705 (2022).

[58] A. Parnami and M. Lee, "Learning from Few Examples: A Summary of Approaches to Few-Shot Learning," arXiv (2022), 10.48550/arxiv.2203.04291, 2203.04291.

[59] K. Kaufmann, H. Lane, X. Liu, and K. S. Vecchio, "Efficient few-shot machine learning for classification of EBSD patterns," *Scientific Reports* **11**, 8172 (2021), http://www.nature.com/articles/s41598-021-87557-5.

[60] C. Doty, S. Gallagher, W. Cui, W. Chen, S. Bhushan, M. Oostrom, S. Akers, and S. R. Spurgeon, "Design of a graphical user interface for few-shot machine learning classification of electron microscopy data," *Computational Materials Science* **203**, 111121 (2022-2), https://linkinghub.elsevier.com/retrieve/pii/S0927025621007874, 2107.10387.

[61] M. Olszta, K. Fiedler, D. Hopkins, K. Yano, C. Doty, M. Oostrom, S. Akers, and S. R. Spurgeon, "Pivot Point: The Key to TEM Automation," *Microscopy and Microanalysis* **28**, 2920–2921 (2022).

[62] M. Olszta and K. Fiedler, "Nanocartography: Planning for success in analytical electron microscopy," arXiv (2022), 10.48550/arxiv.2205.03956, 2205.03956.

[63] M. Olszta, K. Fiedler, S. Spurgeon, S. Reehl, and D. Hopkins, "The role of Nanocartography in the Development of Automated TEM," *Microscopy and Microanalysis* **27**, 2986–2987 (2021).

[64] M. Olszta and K. Fiedler, "Nanocartography in the Age of Automated TEM," *Microscopy and Microanalysis* **26**, 32–32 (2020).

[65] D. A. Muller and M. J. Mills, "Electron microscopy: probing the atomic structure and chemistry of grain boundaries, interfaces and defects," *Materials Science and Engineering: A* **260**, 12–28 (1999).

[66] JEOL, "PyJEM Software Package, Available at https://github.com/PyJEM/PyJEM," (2023).

[67] Y. Gong, Y. Dong, B. Zhao, R. Yu, S. Hu, and Z. Tan, "Diverse applications of MoO$_3$ for high performance organic photovoltaics: fundamentals, processes and optimization strategies," *Journal of Materials Chemistry A* **8**, 978–1009 (2019).

[68] C. Robertson, J. L. Wilmoth, S. Retterer, and M. Fuentes-Cabrera, "Performing Video Frame Prediction of Microbial Growth with a Recurrent Neural Network," arXiv, 1–15 (2022), 2205.05810.

[69] N. R. Lewis, Y. Jin, X. Tang, V. Shah, C. Doty, B. E. Matthews, S. Akers, and S. R. Spurgeon, "Forecasting of in situ electron energy loss spectroscopy," npj *Computational Materials* **8**, 252 (2022).